Comparison of Color Doppler Ultrasound Characteristics between Parotid Mucoepidermoid Carcinoma and Basal Cell Adenoma

Shubao Chen1, Size Wu2*

¹Department of Ultrasonography, Hainan General Hospital (Hainan Affiliated Hospital of Hainan Medical University), Haikou, China, ²Department of Ultrasound, The First Affiliated Hospital of Hainan Medical University, Haikou, China

Abstract

Knowledge of the color Doppler ultrasound (US) characteristics of parotid malignant mucoepidermoid carcinoma and benign basal cell adenoma remains limited. To enhance understanding of these two diseases, we retrospectively analyzed 9 cases of surgically and histopathologically confirmed mucoepidermoid carcinomas and 18 cases of basal cell adenomas. The results revealed that mucoepidermoid carcinomas exhibited irregular and deeply lobulated shapes in 55.5% of cases, ambiguous margins in 88.8%, and punctuate calcifications in 66.7%. In contrast, basal cell adenomas demonstrated regular and shallowly lobulated shapes in 72.2% of cases, clear margins in 100%, and calcifications in only 5.6%. Significant differences were observed in these characteristics between the two tumor types. Therefore, we conclude that the color Doppler US features closely associated with mucoepidermoid carcinoma include deeply lobulated or irregular shapes, ambiguous margins, and punctate calcifications. Recognizing these characteristics can facilitate the differential diagnosis of the two kinds of tumors.

Keywords: Basal cell adenoma, color Doppler ultrasound, mucoepidermoid carcinoma, parotid glands

INTRODUCTION

The parotid gland is a superficial organ located anterior to the ear and the sternocleidomastoid muscle, comprising a superficial lobe and a deep lobe separated by the plane through which the facial nerve and its branches traverse, situated in the retromandibular fossa.[1] Tumors and other diseases can occur in the parotid gland, whereas treatment and prognosis for benign and malignant tumors are different. Inaccurate diagnosis and treatment of malignant tumors can lead to severe consequences.^[2-6] Therefore, accurate diagnosis is crucial for treatment planning. The gold standard for diagnosing parotid tumors is histological biopsy, whereas noninvasive imaging assessments are predominantly performed using magnetic resonance imaging (MRI) and computed tomography (CT). Among primary malignant parotid tumors, mucoepidermoid carcinoma is the most common and needs to be distinguished from benign parotid tumors such as Warthin's tumors, pleomorphic adenomas,

Received: 22-11-2024 Revised: 01-01-2025 Accepted: 09-03-2025 Available Online: 18-09-2025

Access this article online

Quick Response Code:

Website:
https://journals.lww.com/jmut

DOI:
10.4103/jmu.JMU-D-24-00020

and basal cell adenomas, among others.^[3-8] CT can provide a comprehensive view of the parotid gland and the tumor, reveal adjacent bone and deep tissues, and sensitively detect calcifications within the tumor.^[9,10] MRI offers excellent soft-tissue resolution, enabling visualization of the margins and regional metastasis of malignant parotid tumors, as well as the relationship of the tumor to the facial nerve.^[11,12] However, in routine clinical practice, color Doppler ultrasound (US) remains the preferred first-line imaging modality due to its convenience, free from ionizing radiation, cost-effectiveness, and overall good diagnostic performance. It excels in identifying the cystic and solid components of parotid tumors, detecting vascularity, and measuring tumor size. A comprehensive understanding of the US characteristics of parotid lesions is essential for accurate

Address for correspondence: Prof. Size Wu, Department of Ultrasound, The First Affiliated Hospital of Hainan Medical University, No. 31, Longhua Road, Haikou 570102, China. E-mail: wsz074@aliyun.com

This is an open access journal, and articles are distributed under the terms of the Creative Commons Attribution-NonCommercial-ShareAlike 4.0 License, which allows others to remix, tweak, and build upon the work non-commercially, as long as appropriate credit is given and the new creations are licensed under the identical terms.

 $\textbf{For reprints contact:} \ WKHLRPMedknow_reprints@wolterskluwer.com$

How to cite this article: Chen S, Wu S. Comparison of color Doppler ultrasound characteristics between parotid mucoepidermoid carcinoma and basal cell adenoma. J Med Ultrasound 2025;33:260-5.

Abbreviations

CT Computed tomography

MHz Megahertz

MRI Magnetic resonance imaging

PACS Picture archiving and communication system SPSS Statistical product and service solutions

US Ultrasound

diagnosis. While the US features of Warthin's tumors and pleomorphic adenomas have been extensively studied, [7,8,13] there is a paucity of research on the US characteristics of the relatively rare mucoepidermoid carcinoma and basal cell adenoma, warranting further investigation. [3,4] Although basal cell adenomas are typically benign, they can be misdiagnosed as mucoepidermoid carcinoma. They can undergo malignant transformation, and therefore, a differential diagnosis should not be overlooked. [2,5,14] The aim of this study was to analyze the US characteristics of parotid mucoepidermoid carcinoma, compare them with those of basal cell adenoma, and enhance understanding of these diseases.

MATERIALS AND METHODS

Study population

In this retrospective study, data from patients who underwent the US for parotid gland evaluation and subsequently underwent surgical resection of parotid tumors at Hainan General Hospital between January 1, 2019, and December 31, 2023, were retrospectively reviewed. US images of the parotid tumors and relevant patient data were collected and analyzed. The inclusion criteria for the study were as follows: (1) postoperative pathology confirming parotid basal cell adenoma or parotid mucoepidermoid carcinoma; (2) patients who had not received prior treatment for parotid lesions before undergoing US examination; and (3) patients with complete clinical data. The exclusion criteria for the study were: (1) patients with more than two pathological types present in the same tumor and (2) patients with poor-quality US images of the parotid lesion or incomplete visualization of parotid lesions, hindering reanalysis. This study received approval from the Ethics Committee of Hainan General Hospital with (approval number: (2024)159; approval date: 02/28/2024). Patient informed consent requirements were waived due to the retrospective nature of the study and in accordance with relevant regulations. The data obtained from patients who had undergone procedures of US evaluation, biopsy, and/ or surgical operation, and all procedures followed were in accordance with the ethical standards of the responsible committee on human experimentation (institutional and national) and with the World Medical Association Declaration of Helsinki (revised in 2013).

Color Doppler ultrasound examination

The US examinations of the parotid glands were conducted by 9 US physicians with over 3 years of experience. The US physicians followed a standardized protocol for Doppler US imaging to minimize variability. The US systems used for evaluating patients with parotid lesions were Toshiba Aplio 500 (Toshiba Medical Systems, Tokyo, Japan), Mylab Twice eHD (Esaote S.p.A., Genoa, Italy), and Mindray DC8 (Shenzhen Mindray Bio-Medical Electronics Co., Ltd., Shenzhen, China). During the US examination, patients were positioned supine on a table with a neck pillow to fully expose the face and mandible. Coupling gel was applied to the parotid gland regions, and high-frequency US transducers with operating frequencies of 8–15 MHz were used to scan the parotid glands. If a focal lesion was identified in the parotid gland, the location, shape, margin, internal cystic and solid components, punctate hyperechoic foci, posterior acoustic features, vascularity, and ipsilateral cervical lymph nodes with suspicious metastatic features were documented. Representative US images were saved in the Picture Archiving and Communication System (PACS). Calcifications (punctate hyperechoic foci) < 1 mm were classified as punctate calcifications (also refers to microcalcifications), whereas those >3 mm were considered macrocalcifications. The vascularity distribution in the parotid lesion was categorized based on the number of color signals rendered by color Doppler flow imaging: (1) absence of vascularity, referring to no color signal; (2) scarcity of vascularity, referring to one point-like or piece of color signal; (3) moderate vascularity, referring to two or three point-like and pieces of color signal; and (4) abundant vascularity, referring to three or more point-like and pieces of color signal. For identifying cervical lymph nodes, features such as a length-to-width ratio <2, loss of hilum, punctate hyperechoic foci, and anechoic liquefaction were indicative of suspicious metastasis. In this study, a junior US physician initially searched the PACS for patients with histopathologically confirmed parotid mucoepidermoid carcinoma and basal cell adenoma. Subsequently, the corresponding US images of the parotid lesions and relevant information were retrieved and saved to a portable digital disk. The US features of the parotid lesions were independently analyzed by two US physicians with over 5 years of experience in evaluating superficial organs and tissues. These physicians were blinded to previous US diagnoses and pathological results. In cases where the two physicians disagreed on the interpretation of a parotid lesion, a third US physician with 17 years of experience was consulted. If multiple parotid lesions were present, only the largest lesion or the one suspected to be malignant was included for analysis.

Statistical analysis

Continuous variables were assessed for normality using the Shapiro–Wilk test. If the age of patients and the size of parotid lesions followed a normal distribution, they were presented as mean ± standard deviation and analyzed using the independent samples *t*-test. Categorical data were presented as counts and percentages. The Chi-square test and Fisher's exact test were utilized for analyzing categorical data based on the appropriate conditions. Ordinal data were analyzed using the Mann–Whitney *U*-test. Statistical analysis was conducted

using SPSS statistical software version 26.0 (IBM Corp., Armonk, NY, USA), with a two-tailed P < 0.05 considered statistically significant.

RESULTS

A total of 27 patients were included in this study after excluding five patients with mucoepidermoid carcinoma and two patients with basal cell adenoma. Among them, 9 patients had mucoepidermoid carcinoma, and 18 patients had basal cell adenoma. In the group of patients with mucoepidermoid carcinoma, there were 3 males and 6 females, with ages ranging from 23 to 62 years. In the group of patients with basal cell adenoma, there were 6 males and 12 females, with ages ranging from 25 to 72 years. The difference in age between the patients with mucoepidermoid carcinoma and basal cell adenoma was significant (P < 0.05). The sizes of mucoepidermoid carcinoma and basal cell adenoma were similar, with no significant difference between them (P > 0.05). Details of the patient's age, sex, and tumor size are provided

in Table 1. Mucoepidermoid carcinomas were characterized by a combination of irregular and deeply lobulated shapes in 55.5% of cases, ambiguous margins in 88.8%, and punctate calcifications in 66.7% of cases. Basal cell adenomas exhibited regular and shallowly lobulated shapes in 72.2% of cases, clear margins in 100% of cases, and punctate calcifications in a few cases (5.6%). Significant differences were observed in these characteristics between the two diseases (all P < 0.05). Further details are presented in Table 1. Figures 1–4 depict the US characteristics of mucoepidermoid carcinoma and basal cell adenoma, respectively.

DISCUSSION

The US characteristics of 9 parotid mucoepidermoid carcinomas and 18 basal cell adenomas, along with associated demographic information, were summarized and compared in this study. Mucoepidermoid carcinomas were observed in younger individuals, whereas basal cell adenomas occurred in older individuals, with both types predominantly affecting

Characteristic	Basal cell adenoma ($n=18$), n (%)	Mucoepidermoid carcinoma $(n=9)$, n (%)	P
Sex			
Male	6 (33.3)	3 (33.3)	0.672
Female	12 (66.7)	6 (66.7)	
Age (year)	53.3±12.9	37.44 ± 13.0	0.006
Maximal diameter (mm)	23.3±7.4	20.7±5.9	0.368
Shape			
Round/ovoid/elliptic	9 (50.0)	2 (22.2)	0.044
Shallow lobulated	4 (22.2)	2 (22.2)	
Deep lobulated	5 (27.8)	1 (11.1)	
Irregular	0	4 (44.4)	
Margin			
Circumscribed	18 (100)	1 (11.1)	< 0.001
Ambiguous	0	8 (88.9)	
Composition			
Mixture of solid and liquid	6 (33.3)	4 (44.4)	0.683
Solid	12 (66.70)	5 (55.6)	
Texture			
Homogeneous	8 (44.4)	2 (22.2)	0.406
Heterogeneous	10 (55.6)	7 (77.8)	
Punctate hyperechoic			
Absent	17 (94.4)	3 (33.3)	0.002
Present	1 (5.6)	6 (66.7)	
Posterior acoustic feature			
Enhancement	18 (100.0)	8 (88.9)	0.333
No evident change	0	0	
Attenuation	0	1 (11.1)	
Vascularity		· ,	
A few	5 (27.8)	4 (44.4)	0.34
Intermediate	11 (61.1)	5 (55.6)	
Abundant	2 (11.1)	0	
Cervical lymph node of suspicious metastasis	. ,		
No	18 (100.0)	7 (77.8)	0.103
Yes	0	2 (22.2)	

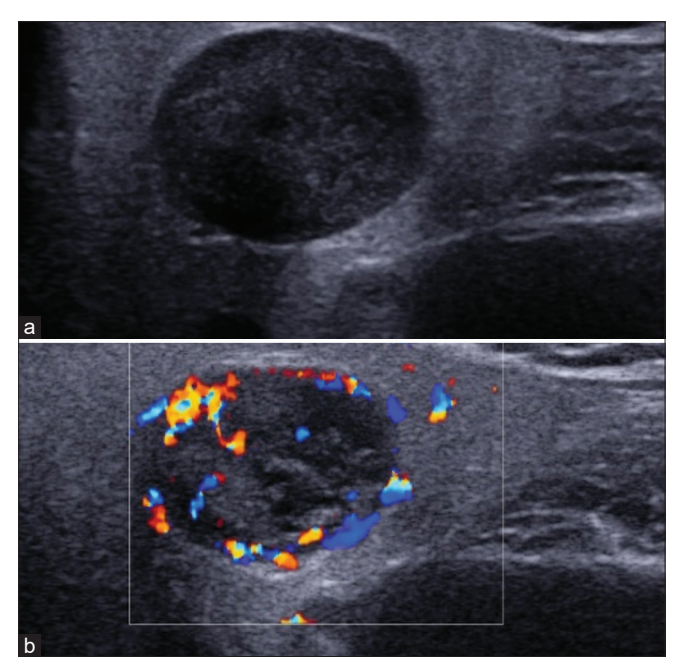


Figure 1: A 35-year-old man with a basal cell adenoma in the right parotid gland. (a) The tumor is ovoid in shape, with circumscribed margin, scattered small anechoic areas, and enhanced posterior echoes, (b) color Doppler flow imaging shows the tumor has rich vascularity

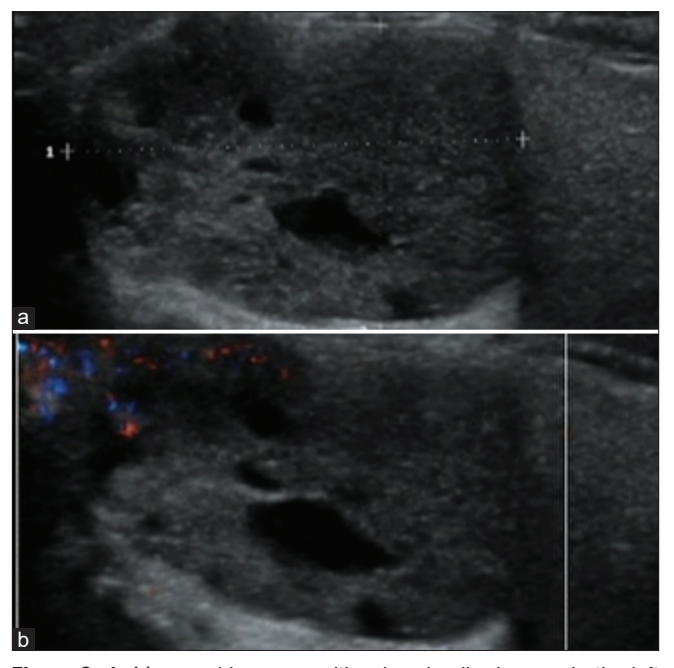


Figure 3: A 44-year-old woman with a basal cell adenoma in the left parotid gland. (a) The tumor presents deep lobulated shape, with scattered anechoic areas and enhanced posterior echoes, (b) color Doppler flow imaging shows the tumor has a few vascularity

women. These findings are consistent with previous studies.^[2-6] The US characteristics of the two parotid tumors were generally in line with previous studies.^[2,15,16] Interestingly, there was no difference in the presence of enlarged abnormal cervical lymph nodes between patients with the two parotid tumors, contrary to common expectations. This discrepancy may be attributed to

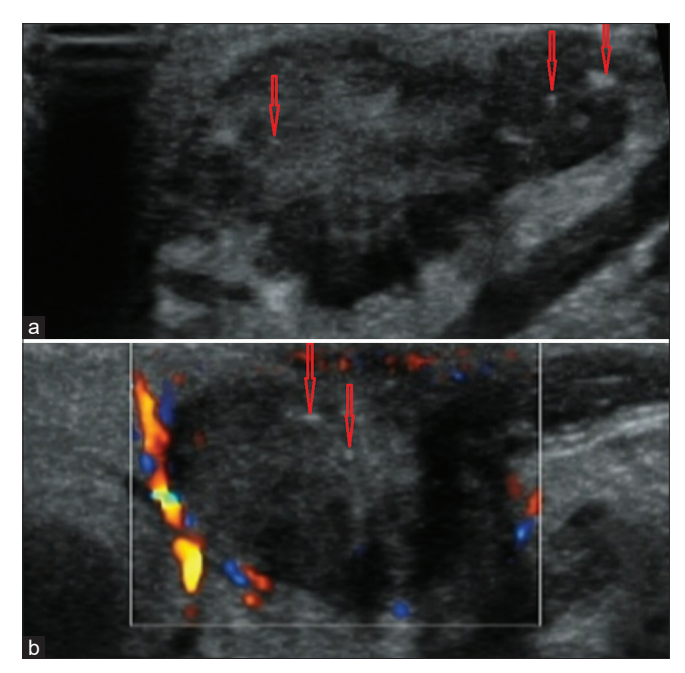


Figure 2: A 62-year-old man with a mucoepidermoid carcinoma in the left parotid gland. (a) The tumor is irregular in shape, with ill-defined margin, several punctate hyperechoic foci (microcalcifications), with partial posterior acoustic shadowing, (b) color Doppler flow imaging shows the tumor has a few vascularity. Red arrows indicate microcalcifications

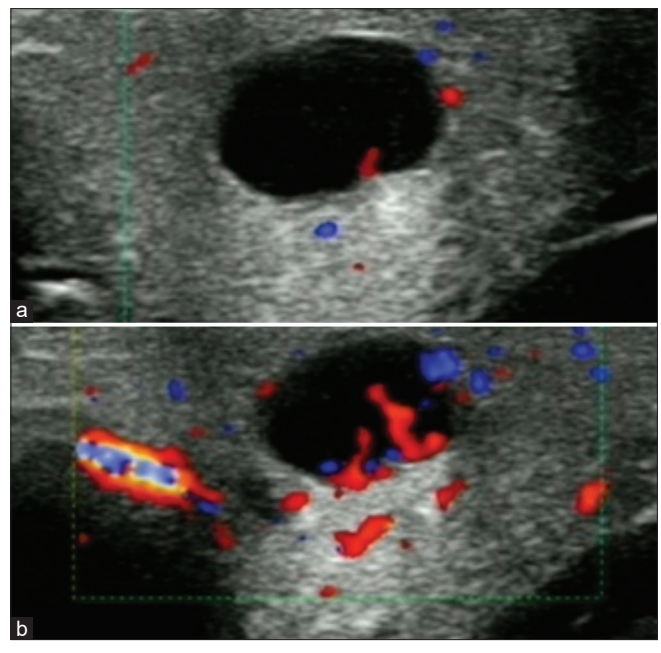


Figure 4: A 7-year-old man with a mucoepidermoid carcinoma in the right parotid gland. (a) The tumor is ovoid in shape, with circumscribed margin and enhanced posterior echoes, (b) color Doppler flow imaging shows the tumor has intermediate vascularity

the small sample size of mucoepidermoid carcinomas with only a few cases of cervical lymph node metastasis, whereas patients with basal cell adenoma may have concurrent benign enlarged cervical lymph nodes. Benign and malignant parotid tumors can undergo degeneration, necrosis, and other pathological changes leading to cystic alterations (liquefying), which can impact the echogenicity and posterior acoustic features of the tumor. The depth, size, and vascularity of parotid lesions in each patient can vary, resulting in diverse US characteristics. In this study, punctate calcifications were identified in 66.7% of mucoepidermoid carcinomas and 5.6% of basal cell adenomas. This finding aligns with a report by Lee et al. that punctate calcifications are present in 10.5% of basal cell adenomas.[17] The incidence of punctate calcifications in mucoepidermoid carcinoma in this study was higher than the 12.2% reported by Gong et al.[3] Therefore, the presence of hyperechoic punctate calcifications within the tumor serves as a crucial feature distinguishing mucoepidermoid carcinoma from basal cell adenoma. In this study, the incidence of punctate calcifications was higher than previously reported for mucoepidermoid carcinoma but lower for basal cell adenoma. This discrepancy may be due to oversight or inadequate awareness among the previous examiners regarding the presence of punctate calcifications and the limited sensitivity of US systems in detecting punctate hyperechoic foci within parotid tumors.^[18] Punctate calcification includes psammoma bodies and other causes associated with calcification. Psammoma bodies are concentric lamellated calcified structures, observed most commonly in papillary thyroid carcinoma and several other malignant tumors, and sometimes in benign lesions, such as serous papillary cystadenoma of the ovary and meningiomas; but seldom reported in other benign tumors and parotid malignant tumors.[19,20] The reason that punctate calcifications are observed more in malignant tumors than benign tumors may be that there are more psammoma bodies in these tumors and further research is required. There were no significant differences between mucoepidermoid carcinoma and basal cell adenoma in terms of composition, texture, and posterior acoustic features, indicating some significant similarities between them that may pose challenges in differential diagnosis.

In summary, the US characteristics of parotid mucoepidermoid carcinoma typically present as a combination of deep lobulated and irregularly shaped entities often with an ambiguous margin, punctate calcifications, and potential presence of ipsilateral cervical enlarged abnormal lymph nodes. On the other hand, the US characteristics of parotid basal cell adenoma commonly manifest as a round or elliptic solid or cystic-solid entity with a circumscribed margin and occasional punctate calcifications. All of them present solid or a mixture of solid and liquid composition, texture, posterior acoustic enhancement, and more or less vascularity.

In the future, in the evaluation of parotid lesions, US elastography and contrast-enhanced US may be used as additional items, for US elastography can reveal the stiffness of parotid tumor and may provide more information for the identification of malignant parotid tumor which is usually more stiffer than benign tumor.^[21-23] Contrast-enhanced US can display the blood perfusion and features of the parotid tumors,

can confirm the presence of liquefied region and necrotized region of the parotid lesions, and can help distinguish malignant parotid tumors from benign parotid tumors. [23,24] For some complex parotid lesions, a combination of color Doppler US findings and CT or MRI findings is necessary, which can obtain more rich information of the parotid lesions and their peripheral condition, improve diagnostic efficacy, and provide information for clinical management. In addition, patient's lifestyle and ethnic features should be considered during the parotid evaluation, for smoking, betel-nut chewing, and so on can affect the well-being of the parotid glands and may induce tumors and associated diseases. [25]

Some limitations exist in this study: (1) The retrospective study design and single-center data collection may introduce sample selection bias; (2) Absence of patient's clinical manifestations and correlation analysis, such as pain, tumor size doubling time; and precipitating factors, such as smoking, alcohol consumption, betel-nut chewing, and radiation exposure; (3) Interobserver agreement of the color Doppler US images acquired by different US systems and physicians were not studied; and (4) The small sample size and absence of atypical cases may limit the generalizability of the findings.^[26,27]

CONCLUSION

Significant differences in US characteristics exist between parotid mucoepidermoid carcinoma and basal cell adenoma. The distinct features associated with parotid mucoepidermoid carcinoma include a combination of deep lobulated and irregular shapes, ambiguous margin, and punctate calcifications. Understanding these characteristics can aid in the differential diagnosis of the two kinds of parotid tumors.

Financial support and sponsorship

Nil.

Conflicts of interest

There are no conflicts of interest.

REFERENCES

- Park HJ, Hong SO, Kim HM, Oh W, Kim HJ. Positional deformation of the parotid gland: Application to minimally invasive procedures. Clin Anat 2022;35:1147-51.
- Hellquist H, Paiva-Correia A, Vander Poorten V, Quer M, Hernandez-Prera JC, Andreasen S, et al. Analysis of the clinical relevance of histological classification of benign epithelial salivary gland tumours. Adv Ther 2019;36:1950-74.
- Gong X, Xiong P, Liu S, Xu Q, Chen Y. Ultrasonographic appearances of mucoepidermoid carcinoma of the salivary glands. Oral Surg Oral Med Oral Pathol Oral Radiol 2012;114:382-7.
- Peraza A, Gómez R, Beltran J, Amarista FJ. Mucoepidermoid carcinoma. An update and review of the literature. J Stomatol Oral Maxillofac Surg 2020;121:713-20.
- Nagao T, Sugano I, Ishida Y, Matsuzaki O, Konno A, Kondo Y, et al. Carcinoma in basal cell adenoma of the parotid gland. Pathol Res Pract 1997:193:171-8.
- Garrett SL, Trott K, Sebastiano C, Wolf MJ, Rao NK, Curry JM, et al. Sensitivity of fine-needle aspiration and imaging modalities in the diagnosis of low-grade mucoepidermoid carcinoma of the parotid gland. Ann Otol Rhinol Laryngol 2019;128:755-9.

- Rong X, Zhu Q, Ji H, Li J, Huang H. Differentiation of pleomorphic adenoma and Warthin's tumor of the parotid gland: Ultrasonographic features. Acta Radiol 2014;55:1203-9.
- Miao LY, Xue H, Ge HY, Wang JR, Jia JW, Cui LG. Differentiation of pleomorphic adenoma and Warthin's tumour of the salivary gland: Is long-to-short diameter ratio a useful parameter? Clin Radiol 2015;70:1212-9.
- Zuo H. The clinical characteristics and CT findings of parotid and submandibular gland tumours. J Oncol 2021;2021:8874100.
- Niazi M, Mohammadzadeh M, Aghazadeh K, Sharifian H, Karimi E, Shakiba M, et al. Perfusion computed tomography scan imaging in differentiation of benign from malignant parotid lesions. Int Arch Otorhinolaryngol 2020;24:e160-9.
- Coudert H, Mirafzal S, Dissard A, Boyer L, Montoriol PF. Multiparametric magnetic resonance imaging of parotid tumors: A systematic review. Diagn Interv Imaging 2021;102:121-30.
- Huang N, Chen Y, She D, Xing Z, Chen T, Cao D. Diffusion kurtosis imaging and dynamic contrast-enhanced MRI for the differentiation of parotid gland tumors. Eur Radiol 2022;32:2748-59.
- Matsuda E, Fukuhara T, Donishi R, Kawamoto K, Hirooka Y, Takeuchi H.
 Usefulness of a novel ultrasonographic classification based on anechoic area patterns for differentiating Warthin tumors from pleomorphic adenomas of the parotid gland. Yonago Acta Med 2017;60:220-6.
- Hage N, Balaji R, Singh NK, Sivakoti S, Shrinivas SB. Basal cell adenoma of the deep lobe of the parotid gland misdiagnosed as mucoepidermoid carcinoma – A case report. Int J Surg Case Rep 2024;123:110218.
- Shi L, Wang YX, Yu C, Zhao F, Kuang PD, Shao GL. CT and ultrasound features of basal cell adenoma of the parotid gland: A report of 22 cases with pathologic correlation. Am J Neuroradiol 2012;33:434-8.
- Kawata R, Yoshimura K, Lee K, Araki M, Takenaka H, Tsuji M. Basal cell adenoma of the parotid gland: A clinicopathological study of nine cases – Basal cell adenoma versus pleomorphic adenoma and Warthin's tumor. Eur Arch Otorhinolaryngol 2010;267:779-83.
- 17. Lee JY, Kim HJ, Kim YK, Cha J, Kim ST. Basal cell adenoma and

- myoepithelioma of the parotid gland: Patterns of enhancement at two-phase CT in comparison with Warthin tumor. Diagn Interv Radiol 2019;25:285-90.
- Zajkowski P, Ochal-Choińska A. Standards for the assessment of salivary glands – An update. J Ultrason 2016;16:175-90.
- Das DK. Psammoma body: A product of dystrophic calcification or of a biologically active process that aims at limiting the growth and spread of tumor? Diagn Cytopathol 2009;37:534-41.
- Negahban S, Daneshbod Y, Khademi B, Seif I. Papillary cystic acinic cell carcinoma with many psammoma bodies, so-called psammoma body-rich papillary cystic acinic cell carcinoma: Report of a case with fine needle aspiration findings. Acta Cytol 2009;53:440-4.
- Matsuda E, Fukuhara T, Donishi R, Taira K, Koyama S, Morisaki T, et al. Clinical utility of qualitative elastography using acoustic radiation force impulse for differentiating benign from malignant salivary gland tumors. Ultrasound Med Biol 2021;47:279-87.
- Heřman J, Sedláčková Z, Vachutka J, Fürst T, Salzman R, Vomáčka J, et al. Differential diagnosis of parotid gland tumors: Role of shear wave elastography. Biomed Res Int 2017;2017:9234672.
- Shi L, Wu D, Yang X, Yan C, Huang P. Contrast-enhanced ultrasound and strain elastography for differentiating benign and malignant parotid tumors. Ultraschall Med 2023;44:419-27.
- Sultan SR, AlKharaiji M, Rajab SH. Diagnosis of parotid gland tumours with contrast-enhanced ultrasound: A systematic review and meta-analysis. Med Ultrason 2022;24:211-8.
- Hassan N, Almaasfeh S, Musa M, Alghamdi S, Abukonna A. Sonographic assessment of the salivary glands among Sudanese snuff-dippers. J Med Ultrasound 2023;31:228-31.
- Balasubiramaniyan V, Sultania M, Sable M, Muduly D, Kar M. Warthin-like mucoepidermoid carcinoma of the parotid gland: A diagnostic and therapeutic dilemma. Autops Case Rep 2019:9:e2019122.
- Heavner SB, Shah RB, Moyer JS. Sclerosing mucoepidermoid carcinoma of the parotid gland. Eur Arch Otorhinolaryngol 2006;263:955-9.